Fesselin, a Synaptopodin-like Protein, Stimulates Actin Nucleation and Polymerization†

Brent Beall and Joseph M. Chalovich*

School of Medicine, East Carolina University, Greenville, North Carolina 27858-4354

Received September 17, 2001

ABSTRACT: Fesselin is a proline-rich actin binding protein that has recently been isolated from smooth muscle [Leinweber, B. D., Fredricksen, R. S., Hoffman, D. R., and Chalovich, J. M. (1999) *J. Muscle Res. Cell Motil. 20*, 539−545]. Fesselin is similar to synaptopodin [Mundel, P., Heid, H. W., Mundel, T. M., Krüger, M., Reiser, J., and Kriz, W. (1997) *J. Cell Biol. 139*, 193−204] in terms of its size, isoelectric point, and sequence although synaptopodin is not present in smooth muscle. The function of fesselin is unknown. Evidence is presented here that fesselin accelerates the polymerization of actin. Fesselin was effective on actin isolated from either smooth or skeletal muscle at low ionic strength and in the presence of 100 mM KCl. At low ionic strength, fesselin decreased the time for 50% polymerization to about 1% of that in the absence of fesselin. The lag phase characteristic of the slow nucleation process of polymerization was eliminated as the fesselin concentration was increased from very low levels. Fesselin did not alter the critical concentration for actin but did increase the rate of elongation by ≈3-fold. The increase in elongation rate constant is insufficient to account for the total increase in polymerization rate. It is likely that fesselin stabilizes the formation of actin nuclei. Time courses of actin polymerization at varied fesselin concentrations and varied actin concentrations were simulated by increasing the rate of nucleation and both the forward and reverse rate constants for elongation.

Fesselin is an actin binding protein that has recently been isolated from turkey gizzard muscle (*1*). Fesselin is noteworthy because of its potent ability to bundle actin and because of its similarity to synaptopodin, a protein found in telencephalic dendrites and renal podocytes but not in smooth muscle (*2*). Fesselin has in common with synaptopodin a similar p*I* (9.3), a similar mobility on SDS gels (103 and 79 kDa for fesselin and 110 kDa for synaptopodin), a high proline content, and regions of sequence homology. Antibodies directed against synaptopodin decorate actin filaments in cells forming a punctate pattern (*2*); this pattern is lost following depolymerization of actin with cytochalasin B. Preliminary studies with fesselin also indicate that fesselin co-localizes with α-actinin on actin filaments (*3*). The functions of fesselin and synaptopodin are unknown.

The effect of fesselin on actin polymerization was examined because of its ability to bind to and bundle actin filaments and its high isoelectric point. The isoelectric point was a consideration because cationic substances tend to polymerize actin (*4*, *5*). Actin binding and polymerizing proteins are often basic (*6*), and charge neutralization may be a factor in the function of these proteins (*5*).

The present study provides evidence that fesselin increases the rate of actin polymerization. This was seen by increases in the apparent rates of increase of both pyrene fluorescence and light scattering and decrease of intrinsic tryptophan fluorescence. Except at the lowest concentrations of fesselin examined, the lag phase of actin polymerization was eliminated. Fesselin was effective on both skeletal and smooth muscle actin at low and moderate ionic strength. The 103 and 79 kDa forms of fesselin were separated, and both forms were shown to be active. The activity of fesselin is comparable to that of other proteins that are thought to modulate actin filament dynamics (*7*−*12*). Fesselin did not change the critical concentration of actin. The rate constant for elongation of actin was accelerated about 3-fold, but the major effect of fesselin appeared to be in the rate constant of nucleation. Time courses of actin polymerization in the presence of fesselin measured at varied protein concentrations were simulated by increasing the rate constant of nucleation as well as the forward and reverse rate constants for actin for elongation (giving a constant critical concentration). The abilities of fesselin to organize actin filaments and stimulate polymerization may reflect the cellular function of fesselin and related proteins.

MATERIALS AND METHODS

Protein Preparations. Rabbit muscle G-actin was purified using the method of Spudich and Watt (*13*) with modifications (*14*) and then further purified by gel-filtration chromatography on a Sephacryl S-200 column (Pharmacia LKB Biotechnology Inc.) in a buffer containing 5 mM Tris, 0.2 mM ATP, 0.5 mM DTT, 0.1 mM $CaCl_2$, and 0.01% NaN_3, pH 7.8 (G-buffer). Pyrene-labeled actin was prepared by reacting F-actin with *N*-(1-pyrenyl)iodoacetamide (Molecular Probes) using the method of Kouyama and Mihashi (*15*). The actin was depolymerized by exhaustive dialysis, clarified by centrifugation, and then purified by gel-filtration chromatography on a Sephacryl S-200 column. The actin concen-

† Funded by NIH Grant AR35216 and a Faculty Research Grant. A preliminary report of this work was presented at the 44th Biophysical Society Meeting, New Orleans, LA (*1*).

* To whom correspondence should be addressed. Fax: 252-816-3383. Phone: 252-816-3383. E-mail: chalovich@brody.med.ecu.edu.

10.1021/bi011806u CCC: $20.00
Published on Web 11/02/2001

tration was determined by absorbance measurements at 290 nm corrected for light scattering at 500 nm using the extinction coefficient of 0.617 mg^{-1} mL cm^{-1} (*15*). The pyrene-actin concentration and the labeling extent were calculated from the absorbance at 290 and 344 nm (*16*). The extent of labeling varied from 0.7 to 0.9 mol/mol. Smooth muscle actin was purified from turkey gizzards using the method of Carsten and Mommaerts (*17*) with some modification (*18*). Prior to use in polymerization assays, the actin was incubated for at least 5 min in the presence of 125 μM EGTA, and 50 μM $MgCl_2$ in order to replace Ca^{2+} in the tight binding site of actin with Mg^{2+} (*19*).

Fesselin was purified from turkey gizzards using the method of Leinweber et al. (*1*). The fesselin concentration was determined by the Lowry assay using bovine serum albumin as a standard. The two fesselin polypeptides were separated by reverse-phase HPLC using a μBondapak C18 column (Waters) at 30 °C and a linear gradient from 30% acetonitrile, 0.1% trifluoroacetic acid to 40% acetonitrile, 0.1% trifluoroacetic acid. The first peak contained the lower molecular weight form of fesselin, while the second peak contained the higher molecular weight form. Fractions containing fesselin were lyophilized and dissolved in water for subsequent analysis. Prior to use, all fesselin solutions were clarified by centrifugation at 100000*g* for 45 min.

Cosedimentation Assay. As a preliminary test of polymerization activity, skeletal muscle G-actin in a buffer containing 5 mM Tris, 0.2 mM ATP, 0.5 mM DTT, 0.1 mM $CaCl_2$, 0.01% NaN_3, and 2 mM $MgCl_2$, pH 7.8 (G-buffer + 2 mM $MgCl_2$), was mixed with fesselin and immediately centrifuged in an Airfuge (Beckman, Fullerton, CA) at 30 000 psi for 30 min. Only polymerized actin or F-actin was sedimented appreciably under these conditions. The pellets of polymerized actin were analyzed quantitatively by SDS−PAGE. Densitometry of Coomassie Blue-stained gels was used to determine the fraction of total actin that was polymerized by fesselin.

Critical Concentration Determination. The critical concentration was determined by the relationship of the extent of actin polymerization to the actin concentration (*7*). Either pyrene-labeled F-actin or unlabeled F-actin was serially diluted into G-buffer or G-buffer containing 2 mM $MgCl_2$ with or without fesselin. The point at which the slope of the plot of fluorescence against the actin concentration increased abruptly gave the critical concentration.

Polymerization Assays. Actin polymerization was monitored either on a Fluorolog 2 spectrofluorometer (Spex) or on an Applied Photophysics DX17.MV/2 sequential mixing stopped-flow spectrophotometer. The stopped-flow device gave much better resolution of the early changes in the reaction, but the fluorometer was preferable for obtaining the end point of very slow reactions. The stopped-flow device also had an over-sampling feature to increase the signal-to-noise ratio. Pyrene actin fluorescence (*21*), intrinsic Trp fluorescence (*22, 23*), and light scattering (*21, 24*) measurements were all employed to ensure that the changes measured were due to polymerization. In all cases, the excitation wavelength (λ_x)[1] was set with a monochromator, and the emission wavelength (λ_m) was set either with a monochromator (conventional fluorometer) or with long-pass filters (stopped-flow). The following excitation and emission wavelengths were used to monitor changes in pyrene fluorescence: $\lambda_x = 344$ nm, $\lambda_m = 366$ nm (*12*); $\lambda_x = 365$ nm, $\lambda_m = 385$ nm (*13*); and $\lambda_x = 365$ nm, $\lambda_m = 407$ nm (*15, 20*). Each method gave the same rate of polymerization although the amplitude of the signal and the extent to which scattered light contributed to the final signal varied with each case. Excitation at 344 nm gave a 4-fold enhancement of fluorescence in going from monomer to polymer. Excitation at 365 nm gave a larger signal (20−25-fold enhancement during polymerization of ≈100% labeled actin), and the signal had a smaller contribution from scattered light. In some pyrene-actin experiments, a paired reaction was run using nonlabeled actin, and this control was subtracted from the curve with pyrene-labeled actin. This correction did not appreciably change the half-time of polymerization but did reduce the amplitude by about 10%. Intrinsic Trp fluorescence was measured with $\lambda_x = 300$ nm and $\lambda_m = 335$ nm. Light scattering was measured with $\lambda_x = \lambda_m = 550$ nm.

Effect of Fesselin on the Rate of Actin Elongation. F-Actin was sonicated at 8 W for 30 s using a sonicator (Tekmar-Dohrmann, Cincinnati, OH) with a 2 mm titanium tip to produce very short actin filaments or "sonicated actin". The sonicated actin was added to G-actin to initiate elongation (*25*). The contribution of sonicated actin to the total actin concentration did not exceed 5%. The sonication method of producing sonicated actin was used to avoid the addition of other substances that may interact with fesselin in an unknown manner. The observed rate of polymerization is approximately given by: $v = v_0 + (k_+[A] + k_-)$[sonicated actin], where v_0 is the polymerization rate in the absence of sonicated actin, k_+ is the sum of the rate constants for elongation at both ends of the actin filament, and k_- is the corresponding rate constant sum for polymer shortening. This equation is true if the number of polymers is determined by the number of short actin filaments added to initiate the reaction. If k_- is smaller than $k_+[A]$, then the slope of the plot of initial velocity against [sonicated actin] has a slope proportional to k_+.

Simulation of the Time Course of Polymerization. The polymerization of actin involves an activation step, the rate-limiting formation of a nucleus consisting of three to four activated actin monomers followed by a rapid elongation phase in which single activated monomers add in a stepwise manner to the filament. An exact description of actin polymerization is difficult because the growth of a single filament involves the addition of hundreds of actin monomers and a population of actin filaments has a distribution of lengths. Several approaches have been taken to represent the polymerization process (*42, 43*). The rate constants obtained depend somewhat on the model chosen, but models are useful for simulating changes in specific processes (*35*). We used an approach based on an analysis by Wegner and Engel (*24*) as modified by Cooper et al. (*27*). With the MLAB modeling program (Civilized Software), it was possible to solve differential equations for the model without making the steady-state assumption for the nucleation process.

The first step in polymerization is the activation of actin, $A_0 = A_1$, with forward rate constant k_1 and reverse rate constant k_2. This activation process is thought to be due to the binding of Mg^{2+} to actin (*27, 28*). We preexchanged the

[1] Abbreviations: λ_x, excitation wavelength; λ_m, emission wavelength; cc, critical concentration.

bound metal before initiating the polymerization reaction so all reactions began with activated actin, A_1. We assumed that nucleation consisted of a two-step addition of activated actin monomers: $A_1 + A_1 = A_2$; $A_1 + A_2 = A_3$. The rate constants describing both reactions were identical (see eqs 2 and 3). The forward rate constant, k_3, had units of M^{-1} s^{-1}, and the reverse rate constant, k_4, had units of s^{-1}. To solve the differential equation describing the time course of A_3, it was necessary to calculate A_4. We made the simplifying assumption that the value of $A_n = A_{n+1}$ (or $A_4 = A_3$) to calculate A_3 (*24*).

Elongation was assumed to occur by addition of activated actin monomers to the nucleus in a stepwise manner with the forward rate constant k_5 (M^{-1} s^{-1}) and the reverse rate constant k_6 (s^{-1}). The rate of elongation was assumed to be equal to the product of the concentration of actin, the concentration of actin filaments of any length (N), and the elongation rate constant (*24*). The rate of shortening was given by the product of N and rate constant k_6. The final result of the model is the time course of the change in the concentration of actin protomers (P) in polymers of all size greater than the nucleus. The value of P increased from 0 to a_{tot} − cc where a_{tot} is the total actin concentration and cc is the critical concentration that was measured separately. In simulations, the rate constants were adjusted so that the time course of P matched that of experimental curves.

Calculation of the time course of the change in actin protomer concentration, P, required calculation of the concentration of actin filaments, N. N was assumed to equal the concentration of nuclei or A_3 (*24*). That is, nuclei were considered to be unstable so that they either broke down to their components or elongated rapidly to form a filament. Another potential pathway for changing the number of filaments is the fragmentation of existing filaments. Fragmentation was not included in the simulations because it appeared to have little effect on the results in the conditions used here. The equations used for the simulations are given below:

activation:

$$dA_0/dt = k_2*A_1 - k_1*A_0 \quad (1)$$

nucleation:

$$dA_2/dt = k_3*A_1\wedge 2 + k_4*A_3 - k_4*A_2 - k_3*A_2*A_1 \quad (2)$$

$$dA_3/dt = A_1*(k_3*A_2 - k_5*A_3) + A_3*(k_5*cc - k_4); \quad (k_5*cc = k_6) \quad (3)$$

actin filament concentration:

$$dN/dt = k_3*A_1*A_2 - k_4*A_3 \quad (4)$$

actin protomer concentration:

$$dP/dt = N*(k_5*A_1 - k_5*cc) \quad (5)$$

conservation of mass:

$$A_1 = A_{tot} - A_0 - 2*A_2 - 3*A_3 - P \quad (6)$$

All simulations were done by varying k_3, k_5, and k_6. The values of the other rate constants were $k_1 = 1 \times 10^6$ s^{-1}, $k_2 = 1 \times 10^{-4}$ s^{-1}, and $k_4 = 500$ s^{-1}.

Effect of Actin Concentration. Results of polymerization in the presence of fesselin and different actin concentrations could be compared only if the fraction of actin bound to fesselin was the same at each actin concentration. It was not feasible to work under saturating concentrations of fesselin, so an arbitrary free fesselin concentration was chosen and the total fesselin concentration was adjusted to maintain the free fesselin concentration constant. The relationship between the bound and free fesselin concentrations was determined by solving the McGhee and von Hippel equation (*45*) using MLAB. The parameters describing the binding of fesselin to actin were determined by Leinweber et al. (*1*). Fesselin binds to a site consisting of 4 actin monomers ($n = 4$) with an association constant $K = 2 \times 10^6$ M^{-1}. Binding of a fesselin molecule adjacent to another bound fesselin is favored by a factor of 1.74 ($\omega = 1.74$).

The size of the actin nucleus was estimated by measuring the dependence of the rate of polymerization on the total actin concentration as described earlier (*28, 44*). The relationship between the time for 50% completion of the reaction ($t_{1/2}$) and the actin concentration is given by eq 7 where ns is the nucleus size and z is a proportionality constant.

$$1/t_{1/2} = z*[\text{actin}]^{-(ns/2)} \quad (7)$$

RESULTS

A sedimentation assay was used as a preliminary test of the ability of fesselin to stimulate actin polymerization. Skeletal muscle G-actin was mixed with fesselin and rapidly centrifuged to pellet any polymerized actin. Figure 1A shows that in the absence of fesselin virtually all of the actin was present in the supernatant, indicating that little polymerization occurred during the time of analysis. In the presence of 100 nM fesselin, an appreciable amount of polymerization occurred as seen by the presence of actin in the pellet.

As shown in Figure 1A (lanes b and f), typical fesselin preparations contain two polypeptide chains. To determine if both of these chains were active in polymerizing actin, they were resolved by reversed phase chromatography and tested. Figure 1B shows time courses of polymerization of smooth muscle pyrene-labeled actin in the absence of fesselin and in the presence of the fesselin mixture or either the 79 or the 103 kDa molecular mass species. The lag in actin polymerization was pronounced in the absence of fesselin (curve 1). Elimination of the lag phase and a large increase in the rate of polymerization occurred either with the mixture of fesselin polypeptides or with the pure 79 and 103 kDa polypeptide chains. Because of the similarity of the two fesselin polypeptides, a mixture of both fesselin forms was used for subsequent studies.

Fesselin was as effective at polymerizing skeletal muscle actin as smooth muscle actin. Figure 2A shows a time course of the change in fluorescence of pyrene-labeled skeletal muscle G-actin following a rapid increase in the concentration of $MgCl_2$ from 0.05 to 2 mM (lower curve) or following the addition of both $MgCl_2$ and fesselin (upper curve). In both cases, actin polymerization was accompanied by a large enhancement of pyrene fluorescence intensity as described earlier (*11*). The data were corrected for changes in light scattering. In the absence of fesselin, the rate of actin

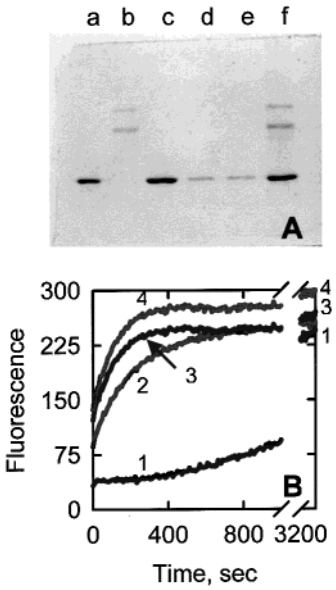

FIGURE 1: Both fesselin polypeptides have actin polymerization activity. (A) SDS−polyacrylamide (7%) gel electrophoresis showing that fesselin promotes actin polymerization. Each assay contained 5 μM skeletal muscle G-actin in 5 mM Tris-HCl, 0.2 mM ATP, 0.5 mM DTT, 0.1 mM $CaCl_2$, and 0.01% NaN_3, pH 7.8. Reactions were initiated by the addition of 2 mM $MgCl_2$ ± 100 nM fesselin and centrifuged immediately in an Airfuge. The supernatants and pellets were analyzed by electrophoresis. (a) Actin standard, (b) fesselin standard, (c) supernatant from $MgCl_2$ alone, (d) pellet from $MgCl_2$ alone, (e) supernatant from $MgCl_2$ + fesselin, (f) pellet from $MgCl_2$ + fesselin. (B) The two fesselin polypeptides seen in panel A were separated by HPLC and tested for the ability to polymerize 5 μM pyrene-labeled smooth muscle actin. Four reactions were monitored simultaneously in a microplate fluorometer. All reactions were initiated by the addition of 2 mM $MgCl_2$ and (1) no fesselin, (2) 0.5 μM 79 kDa polypeptide, (3) 0.5 μM 103 kDa polypeptide, and (4) 0.25 μM of both polypeptides. The cation bound to actin was Mg^{2+} in all reactions.

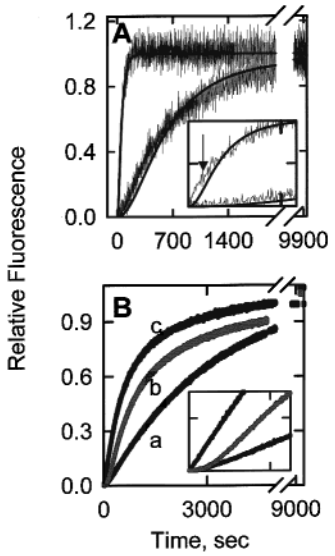

FIGURE 2: Acceleration of pyrene-actin polymerization by fesselin measured by fluorescence changes at 25 °C. (A) Polymerization of 5 μM pyrene-labeled skeletal muscle G-actin in G-buffer containing 2 mM $MgCl_2$ in the absence (lower curve) or presence (upper curve) of 0.5 μM fesselin measured on a spectrofluorometer. The inset shows the initial part of the reaction; the tic marks 150 s. The data were corrected for light scattering by subtracting the curve for an identical reaction run with unlabeled actin. Theoretical curves were generated using eq 1 and the following rate constants: $k_1 = 1 \times 10^6$ s^{-1}, $k_2 = 1 \times 10^{-4}$ s^{-1}, and $k_4 = 500$ s^{-1}. In the absence of fesselin, $k_3 = 5000$ M^{-1} s^{-1} and $k_5 = 10^7$ M^{-1} s^{-1}. In the presence of fesselin, $k_3 = 8.3 \times 10^4$ M^{-1} s^{-1} and $k_5 = 3 \times 10^7$ M^{-1} s^{-1}. The very fast initial part of the curve (see arrow) in the presence of fesselin was presumably due to fesselin binding to G-actin and was not included in the data analysis. (B) Effect of increasing the ionic strength on fesselin-stimulated polymerization. 5 μM skeletal muscle pyrene-labeled actin in G-buffer containing 100 mM KCl and 2 mM $MgCl_2$ was polymerized in the absence of fesselin (a) and in the presence of 1 μM (b) or 2 μM fesselin (c). The inset shows the initial part of the reaction. The tic indicates 450 s. The cation bound to actin was Mg^{2+} in all experiments.

polymerization was characteristically slow and sigmoidal. The lag of about 90 s, most readily seen in the inset, resulted from the rate-limiting formation of actin nuclei. Fesselin caused the elimination of the lag phase and an increase in the rate of polymerization. The theoretical curves shown in Figure 2A were generated by fitting eqs 1−6 to the data. It was assumed that the initial very rapid increase in pyrene fluorescence was due to binding of fesselin to actin; this initial region was not included in the fit. The choice of the rate constants used is described later.

Fesselin retained its activity at higher ionic strength (100 mM KCl and 2 mM $MgCl_2$), but higher concentrations of fesselin were required (Figure 2B). Whether the decreased effectiveness of fesselin was due solely to a reduction in affinity of fesselin for actin or if a reduction in the rate of a subsequent step in polymerization occurred was not determined. The inset to Figure 2B shows that in a manner similar to the low ionic strength condition, sufficiently high concentrations of fesselin eliminated the lag phase of polymerization.

To ensure that the changes reported in Figure 2 were due to polymerization, additional data were collected utilizing light scattering (*21*, *24*) and intrinsic Trp fluorescence (*22*, *23*). In the presence of fesselin, the rate of increase of scattered light intensity was accelerated, and the lag was not observed (data not shown). The intrinsic Trp fluorescence proved to be particularly useful for monitoring actin polymerization by fesselin. The fluorescence decreased by about ~14% upon actin polymerization, and the rate of this decrease was enhanced by fesselin. Figure 3 shows traces of the time course of polymerization of smooth and skeletal muscle actins. Fesselin eliminated the lag phase in both cases. There was no evidence of an initial rapid phase due to binding of fesselin to actin as was observed with pyrene-labeled actin. It is likely that tryptophan fluorescence reflects only polymerization and not the initial binding of fesselin to actin. In contrast to pyrene fluorescence and light scattering, the signal for Trp fluorescence decreased during polymerization. The opposite amplitudes seen for Trp fluorescence compared to light scattering and pyrene fluorescence indicate that each signal is due to actin polymerization. That is, if changes in light scattering dominated the fluorescence signals, an increase in intensity would be observed with every probe or the rates observed would be very different.

The reciprocal of the half-time for polymerization is plotted as a function of the fesselin concentration for each of the probes in Figure 4. Because polymerization time courses were not simple exponential functions, $1/T_{1/2}$ was used as a measure of the rate of the reaction. Both skeletal muscle actin (Figure 3A) and smooth muscle actin (Figure 3B) were studied. All three optical probes give the same

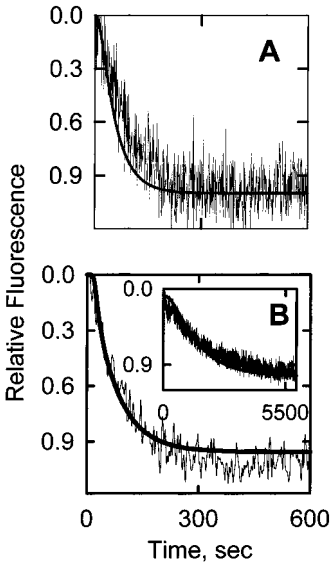

FIGURE 3: Polymerization of 5 μM smooth muscle G-actin (A) and skeletal muscle G-actin (B) measured by Trp fluorescence at pH 7.8 and 25 °C. The actin was initially in G-buffer, and polymerization was initiated by rapidly increasing $MgCl_2$ and fesselin to 0.25 μM. The theoretical curves (solid lines over data) were generated using eqs 1−6 and a series of rate constants. (A) $k_3 = 7.9 \times 10^4$ M^{-1} s^{-1} and $k_5 = 3 \times 10^7$ M^{-1} s^{-1}; (B) $k_3 = 7.9 \times 10^4$ M^{-1} s^{-1} and $k_5 = 3 \times 10^7$ M^{-1} s^{-1}. The cation bound to actin was Mg^{2+} in all experiments. The inset in (B) shows actin polymerization in the absence of fesselin. $k_3 = 3800$ M^{-1} s^{-1} and $k_5 = 1 \times 10^7$ M^{-1} s^{-1}.

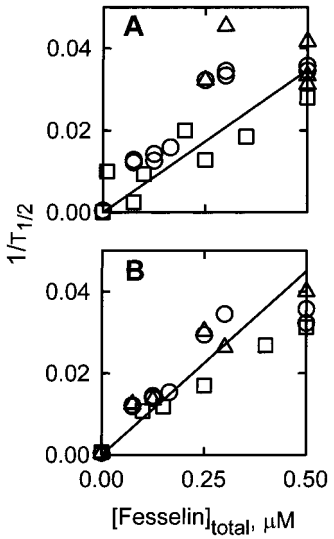

FIGURE 4: Dependence of the rate of polymerization of skeletal (A) and smooth (B) muscle actin on the fesselin concentration. The reciprocal of the time required for 50% of the total signal change for pyrene-actin fluorescence (○), light scattering (△), and intrinsic actin Trp fluorescence (□) is shown as a function of fesselin concentration. The conditions are the same as in Figures 2 and 3.

general result even though in the case of pyrene-actin, the actin was modified. The time required for 50% completion of polymerization decreased ($1/T_{1/2}$ increased) with increasing fesselin concentrations. The time courses of polymerization were unreliable at fesselin concentrations above 0.5 μM because under those conditions the correction for light scattering became significant. As a result, the highest concentration of fesselin used was below that required for stoichiometric binding of fesselin to actin (*1*), and no plateau

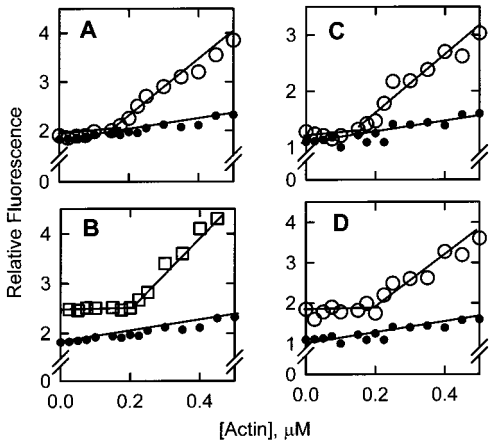

FIGURE 5: Critical concentration of actin in the absence (A and C) and presence of 100 nM fesselin (B and D). Pyrenyl-actin fluorescence was plotted as a function of actin concentration in (A) and (B). Intrinsic Trp fluorescence was plotted as a function of actin concentration in (C) and (D). Trp fluorescence was plotted as an increase in fluorescence for comparison purposes. The values in each sample were fitted by linear regression. The concentration of total unpolymerized actin is given by the break in the fitted curves. G-actin measured in G-actin buffer (solid circles) is shown as a control. The cation bound to actin was Mg^{2+} in all experiments.

in rate was reached. At this standard low ionic strength condition, the lag phase of polymerization was absent even at 75 nM fesselin, and the rate of polymerization was already more than 10 times faster than in the absence of fesselin. At 0.5 μM fesselin, the time for 50% maximum signal was reduced to about 3% of the time required for Mg^{2+} alone irrespective of the source of actin and of the probe used to monitor polymerization.

Several factors might contribute to the acceleration of actin polymerization by fesselin. The critical concentration is that concentration of G-actin in equilibrium with F-actin; below the critical concentration, actin cannot exist as a polymer. The critical concentration is equal to the ratio of the rate constants for polymer chain shortening to the rate constants of polymer chain elongation (*27*, *28*). Figure 5 shows critical concentration measurements made by the net depolymerization of pyrene-labeled F-actin or unlabeled F-actin in either the presence or the absence of fesselin. The fluorescence at equilibrium is shown as a function of the final actin concentration. Actin polymer formation, seen as an increase in pyrene fluorescence or a decrease in intrinsic Trp fluorescence, occurred only when the final actin concentration exceeded the critical concentration. In the absence of fesselin, the break in the curve occurred at approximately 0.17 μM actin, which is in agreement with earlier reports (*26*). In the presence of fesselin, the critical concentration, 0.2 μM, was essentially the same as with pure actin.

The relative elongation rate of actin polymers can be measured by the addition of short actin filaments produced by sonication. The sonicated actin acts as nuclei for elongation. The initial rate of actin polymerization increases in proportion to the concentration of sonicated actin. The slope of the plot of the rate against the sonicated actin concentration is proportional to the rate constant for elongation (*30*). Such a plot is shown in Figure 6 for several fesselin concentrations. The concentration of G-actin + sonicated actin was constant, but the concentration of sonicated actin was at maximum only 5% of the total actin.

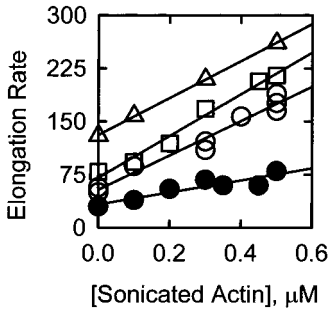

FIGURE 6: Effect of fesselin on the rate of actin polymerization in the presence of actin nuclei. The initial rate of elongation of skeletal G-actin (5 μM) was measured by changes in Trp fluorescence upon polymerization at indicated concentrations of sonicated actin in the absence (closed circles) and presence of 0.01 μM (open circles), 0.075 μM (open squares), or 0.1 μM (open triangles) fesselin. The cation bound to actin was Mg^{2+} in all experiments.

In the absence of fesselin, the addition of sonicated actin eliminated the lag phase (not shown). The rate of polymerization increased in a linear fashion with increasing sonicated actin concentration. The addition of fesselin changed the curve in two ways. First, the rate obtained in the absence of sonicated actin increased with increasing fesselin concentrations as shown earlier. Second, the slope of the plot increased by a factor of ≈3 for all fesselin concentrations between 10 and 100 nM. This 3-fold increase in elongation rate can be compared to the overall acceleration by fesselin of between 5- and 9-fold at these fesselin concentrations. The remaining increase in rate can be attributed to an increase in the rate constant of nucleation.

To determine the effect of fesselin on the rate constant of nucleation, the time courses of polymerization at several fesselin concentrations were simulated. Figure 7A shows sample simulations of three data sets with the elongation rate constant increased by a factor of 3 at all fesselin concentrations. Note that the Trp fluorescence is shown as an increase to facilitate data fitting. The rate of polymer shortening was also increased by a factor of 3 to maintain the same critical concentration. At the lowest fesselin concentration examined here (10 nM), a lag in polymerization is still evident. The duration of the lag decreased with increasing fesselin concentrations. All curves could be simulated by simply adjusting the rate constant for nucleation, k_3. Figure 7B shows the fitted value of the nucleation rate constant as a function of fesselin concentration. The shape of this relationship is not well-defined since the studies at this point were limited to low fesselin concentrations. The nucleation rate constant increased from 3600 s^{-1} in the absence of fesselin to 83 000 s^{-1} in the presence of 250 nM fesselin.

This model was also utilized to simulate the time courses of polymerization as a function of total actin concentration. Polymerization reactions were monitored using Trp fluorescence at the low ionic strength condition with skeletal muscle actin. Several concentrations of actin were examined between 5 and 20 μM. In the absence of fesselin, the rate constants used to simulate the data were similar to those determined by Cooper et al. (*27*). The amount of total fesselin required at each actin concentration to produce 10 nM free fesselin was determined by solving the McGhee and von Hipple equation (*45*), using the affinity of fesselin, and other parameters that were determined earlier (*1*).

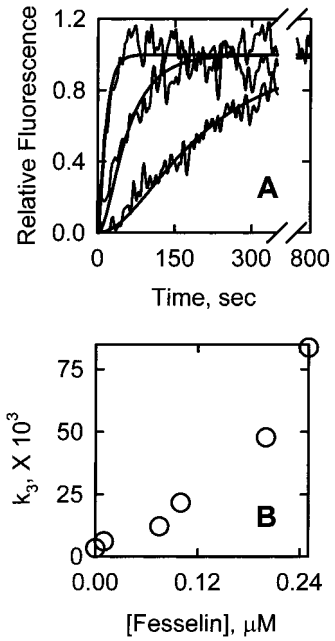

FIGURE 7: Time course of polymerization at several fesselin concentrations monitored by intrinsic Trp fluorescence. Note that the Trp fluorescence is shown as an increase to facilitate data fitting. (A) 5 μM skeletal G-actin was polymerized at 25 °C in the presence of 2 mM $MgCl_2$ and 0.01 μM fesselin (lower curve), 0.1 μM fesselin (middle curve), or 0.25 μM fesselin (upper curve). The theoretical curves were generated using eqs 1−6 and a series of rate constants. For all curves in (A), $k_5 = 3 \times 10^7$ M^{-1} s^{-1}. (Lower curve) $k_3 =$ 6100 M^{-1} s^{-1}; (middle curve) $k_3 = 2.2 \times 10^4$ M^{-1} s^{-1}; (upper curve) $k_3 = 8.3 \times 10^4$ M^{-1} s^{-1}. (B) The rate of nucleation (k_3) is plotted as a function of the concentration of fesselin.

Examples of time courses at various actin concentrations are shown in Figure 8. Again, Trp fluorescence is plotted as an increase to facilitate data analysis. In the absence of fesselin, all curves could be simulated with the same rate constants, the only variable being the actin concentration. Slightly better fits were obtained if the rate constants were allowed to change slightly in the different experiments. Reasonable fits were obtained in the presence of fesselin by assuming a 3-fold increase in the elongation constant and a 2-fold increase in the nucleation rate constant and holding the critical concentration constant. The only variable from one curve to another was the actin concentration.

The relationship between the time for 50% polymerization and the actin concentration has been used to estimate the size of the nucleus. Figure 9 is a plot of $1/T_{1/2}$ against the actin concentration. Equation 7 was fitted to the data to obtain the theoretical curves shown. The nucleus size was approximately 3 both in the absence of fesselin and in the presence of 10 nM fesselin.

DISCUSSION

Actin is required in eukaryotic cells for a host of processes (*29*). The pool of cellular actin must respond rapidly to changes in the environment of the cell. Accessory proteins are available to affect polymerization, severing, bundling, cross-linking, capping, and sequestering of actin (*31, 32*). It is perhaps not too surprising that yet another actin binding protein, fesselin, has been found that modulates actin structural dynamics at least in vitro. Previous work demonstrated that fesselin caused the aggregation of F-actin (*1*).

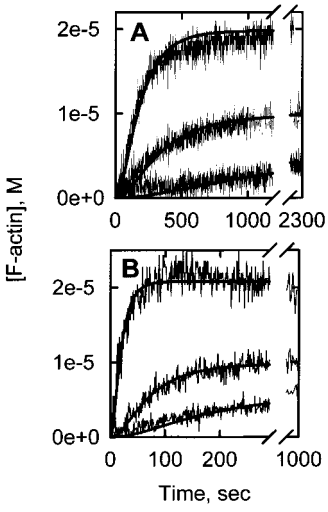

FIGURE 8: Rate of actin polymerization at several actin concentrations in the absence (A) and presence (B) of fesselin. Skeletal G-actin polymerization was monitored at 25 °C using intrinsic Trp fluorescence as a probe. (A) Either 5 μM (lower curve), 10 μM (middle curve), or 20 μM actin (upper curve) was polymerized with 2 mM $MgCl_2$ in G-buffer. The theoretical curves (solid lines over data) were generated using eqs 1−6 and a series of rate constants. For all curves in (A), $k_5 = 1 \times 10^7$ M^{-1} s^{-1}. (Lower curve) $k_3 =$ 3000 M^{-1} s^{-1}; (middle curve) $k_3 = 3100$; (upper curve) $k_3 = 3000$ M^{-1} s^{-1}. (B) 5 μM (lower curve), 10 μM (middle curve), or 20 μM actin (upper curve) was polymerized in the presence of fesselin and 2 mM $MgCl_2$ in G-buffer. At each actin concentration, free fesselin concentration was kept constant at 0.01 μM. The theoretical curves (solid lines over data) were generated using eqs 1−6 and a series of rate constants. For all curves in (B), $k_5 = 3 \times 10^7$ M^{-1} s^{-1}. (Lower curve) $k_3 = 6100$ M^{-1} s^{-1}; (middle curve) $k_3 = 6200$ M^{-1} s^{-1}; (upper curve) $k_3 = 6100$ M^{-1} s^{-1}. Note that the Trp fluorescence is shown as an increase to facilitate data fitting.

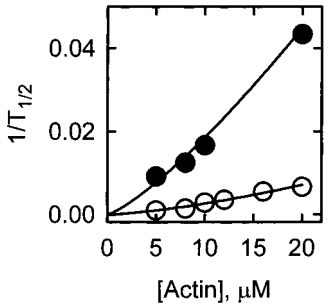

FIGURE 9: Determination of the nucleus size in the absence (open symbols) and presence (closed symbols) of a low concentration of fesselin. The solid curves were calculated from eq 7. The estimated nucleus size was 2.9 in the absence of fesselin and 2.6 in the presence of fesselin.

Together with preliminary evidence showing the localization of fesselin with actin in various tissue preparations (*3*), it is reasonable to suppose that fesselin modulates cellular actin dynamics.

Sedimentation experiments and spectroscopic methods provided evidence that fesselin enhances actin polymerization. Three probes were utilized for the spectroscopic methods to ensure that the observed transition was actin polymerization. Pyrene fluorescence and light scattering both increased with time during polymerization while the intrinsic Trp fluorescence decreased. Thus, while fesselin does cause actin to aggregate into bundles (*1*), this aggregation did not dominate the signals. At fesselin concentrations greater than 500 nM, the aggregation of actin was noticeable, and therefore the experiments shown here were limited to low fesselin concentrations. The apparent rate of polymerization increased with fesselin concentration regardless of the signal used (Figure 3). The time required for 50% polymerization of actin was about 38 times greater in the absence of fesselin than the highest fesselin concentrations used (500 nM) for both skeletal and smooth muscle actin. This degree of acceleration is similar to that reported for other actin binding proteins such as cofilin (*34*).

Fesselin accelerated actin polymerization even in the presence of 100 mM KCl and 2 mM $MgCl_2$. Under these conditions, the affinity of fesselin for actin was apparently lessened so that higher concentrations of fesselin were required to produce a large increase in polymerization rate. At 2 μM fesselin, the half-time for polymerization decreased approximately 3-fold. This is a significant effect when compared to other actin binding proteins. For example, at a lower ionic strength (50 mM KCl and 1 mM $MgCl_2$), 2.3 μM of the Arp 2/3 complex reduced the half-time for polymerization by about 2.5-fold (*8*). In the presence of 150 mM KCl, the polymerizing activity of calponin was almost totally depressed even at calponin concentrations as high as 3 μM (*12*).

We had suggested in our earlier report that the two protein bands in fesselin (79 and 103 kDa) were related to each other as opposed to being two different proteins or two subunits of a single protein (*1*). Using reversed-phase HPLC, the two polypeptides have now been separated, and each enhanced the rate of actin polymerization (Figure 2c).

Fesselin reduced the duration of the lag of polymerization and eliminated it completely at sufficiently high concentrations. The lag phase in the polymerization results from the rate-limiting formation of nuclei consisting of three or four actin monomers (*24*, *27*, *28*, *40*).

Fesselin had a modest effect on the rate of elongation of actin filaments. Fesselin had no effect on the critical concentration defined as the ratio of the sum of the rate constants for shortening at both ends (k_6) to the sum of the rate constants for elongation at the pointed and barbed ends (k_5) (*27*, *28*). Therefore, fesselin must also increase the rate constant for filament shortening. The effect of fesselin on the elongation rate constant was invariant over the range of fesselin concentrations from 10 to 100 nM. The constancy of this effect was unexpected because the effect of fesselin on the polymerization constant was not maximized at this lowest concentration. It is possible that the effect of fesselin on the elongation rate has been overestimated or that there are long-range effects on F-actin that facilitate the addition of actin monomers.

It is clear that the increase in polymerization rate constant is insufficient to explain the large overall effect of fesselin on the rate of polymerization. It was possible to simulate polymerization kinetics as a function of fesselin concentration and actin concentration by assuming that the major effect of high concentrations of fesselin was an increase in the rate constant for nucleation. At the highest fesselin concentration used, the rate of nucleation was 23× that in the absence of fesselin. The rate constant for elongation was increased about 3-fold at all fesselin concentrations examined.

Should the elongation rate constant be overestimated, the effect on the nucleation rate constant would be increased by the same factor. That is, the data could be simulated equally

well without invoking any change in elongation or shortening rate constants as long as the nucleation rate constant was increased proportionately. This emphasizes the point that the simulations shown here are not unique. The simulations show that the suggested role of fesselin is feasible and consistent with experimental results. Other approaches will be required to test this model.

The actin concentration dependence of the polymerization rate was analyzed to estimate the effect of fesselin on the number of actin monomers in a nucleus. The results obtained were done at a low fesselin concentration where the rate of polymerization was only 5-fold greater than in the absence of fesselin. At these conditions, the nucleus size was approximately 3 in each case.

The information obtained thus far suggests that fesselin has some unique properties. Side-binding proteins such as caldesmon (*11*), calponin (*12*), and nebulin fragments (*9*) tend to have a more dramatic effect on the lag phase than capping proteins such as capping protein (*37*, *38*) and cofilin (*35*), although the latter do increase the rate of nucleation. However, none of the above-mentioned proteins have been reported to eliminate the lag phase of polymerization at such low concentrations as observed here for fesselin. Nebulin fragments (*10*) and caldesmon (*12*) both reduce the critical concentration of actin. Capping proteins tend to increase the critical concentration of actin (*7*, *8*, *27*, *28*, *35*, *37*, *38*). Fesselin produced a very small increase in the critical concentration, but the difference may not be significant. These properties, particularly the large increase in the rate constant for nucleation, make fesselin deserving of further study.

ACKNOWLEDGMENT

We thank Mr. Michael Vy-Freedman for assistance with fesselin preparations, Dr. Paul L. Fletcher, Jr., and Ms. Lily K. Fainter for assistance with the HPLC separation of fesselin, the reviewers of this paper for helpful suggestions, and ButterBall of Wallace, NC, for supplying turkey gizzards.

REFERENCES

1. Leinweber, B. D., Fredricksen, R. S., Hoffman, D. R., and Chalovich, J. M. (1999) *J. Muscle Res. Cell Motil. 20*, 539−545.
2. Mundel, P., Heid, H. W., Mundel, T. M., Krüger, M., Reiser, J., and Kriz, W. (1997) *J. Cell Biol. 139*, 193−204.
3. Leinweber, B. D. (1997) Maintaining the Localization of Actin in Smooth Muscle: a-actinin, Filamin, Calponin, and Sm85/Sm95, Ph.D. Thesis, East Carolina University.
4. Bárány, M., Biro, N. A., and Molnar, J. (1955) *Acta Physiol. Acad. Sci. Hung. 5*, 63−78.
5. Tang, J. X., and Janmey, P. A. (1996) *J. Biol. Chem. 271*, 8556−63.
6. Kasai, M., and Oosawa, F. (1969) *Biochim. Biophys. Acta 172*, 300−310.
7. Mullins, R. D., Stafford, W. F., and Pollard, T. D. (1997) *J. Cell Biol. 136*, 331−343.
8. Mullins, R. D., Heuser, J. A., and Pollard, T. D. (1998) *Proc. Natl. Acad. Sci. U.S.A. 95*, 6181−6186.
9. Chen, Mu-Jung G., Shih, C. L., and Wang, K. (1993) *J. Biol. Chem. 268*, 20327−20334.
10. Galazkiewicz, B., Buss, F., Jockusch, B. M., and Dabrowska, R. (1991) *Eur. J. Biochem. 195*, 543−547.
11. Makuch, R., Kulikova, N., Graziewicz, M. A., Nowak, E., and Dabrowska, R. (1994) *Biochim. Biophys. Acta Protein Struct. Mol. Enzymol. 1206*, 49−54.
12. Tang, J. X., Szymanski, P. T., Janmey, P. A., and Tao, T. (1997) *Eur. J. Biochem. 247*, 432−440.
13. Spudich, J. A., and Watt, S. (1971) *J. Biol. Chem. 246*, 4866−4871.
14. Eisenberg, E., and Kielley, W. W. (1971) *Cold Spring Harbor Symp. Quant. Biol. 37*, 145−152.
15. Kouyama, T., and Mihashi, K. (1981) *Eur. J. Biochem. 114*, 33−38.
16. Gordon, D. J., Yang, Y. Z., and Korn, E. D. (1976) *J. Biol. Chem. 251*, 7474−7479.
17. Carsten, M. E., and Mommaerts, W. F. H. M. (1963) *Biochemistry 2*, 28−32.
18. Suzuki, K., Yamaguchi, M., and Sekine, T. (1978) *J. Biochem. (Tokyo) 83*, 869−878.
19. Zimmerle, C. T., Patane, K., and Frieden, C. (1987) *Biochemistry 26*, 6545−6552.
20. Cooper, J. A., Walker, S. B., and Pollard, T. D. (1983) *J. Muscle Res. Cell Motil. 4*, 253−262.
21. Cooper, J. A., and Pollard, T. D. (1982) *Methods Enzymol. 85*, 182−210.
22. Kerwar, G., and Lehrer, S. S. (1972) *Biochemistry 11*, 1211−1217.
23. Selden, L. A., Kinosian, H., Estes, J. E., and Gershman, L. C. (1994) *Adv. Exp. Med. Biol. 358*, 51−57.
24. Wegner, A., and Engel, J. (1975) *Biophys. Chem. 3*, 215−225.
25. Selden, L. A., Kinosian, H. J., Estes, J. E., and Gershman, L. C. (1999) *Biochemistry 38*, 2769−2778.
26. Pollard, T. D. (1986) *J. Cell Biol. 103*, 2747−2754.
27. Cooper, J. A., Buhle, E. L., Jr., Walker, S. B., Tsong, T. Y., and Pollard, T. D. (1983) *Biochemistry 22*, 2193−2202.
28. Tobacman, L. S., and Korn, E. D. (1983) *J. Biol. Chem. 258*, 3207−3214.
29. Frieden, C., Lieberman, D., and Gilbert, H. R. (1980) *J. Biol. Chem. 255*, 8891−8893.
30. Carlier, M.-F., Laurent, V., Santolini, J., Melki, R., Didry, D., Xia, G.-X., Hong, Y., Chua, N.-H., and Pantaloni, D. (1997) *J. Cell Biol. 136*, 1307−1323.
31. Frieden, C. (1982) *J. Biol. Chem. 257*, 2882−2886.
32. Pollard, T. D., and Cooper, J. A. (1986) *Annu. Rev. Biochem. 55*, 987−1035.
33. Carlier, M.-F., Pantaloni, D., and Korn, E. D. (1986) *J. Biol. Chem. 261*, 10778−10784.
34. Zimmerle, C. T., and Frieden, C. (1988) *Biochemistry 27*, 7766−7772.
35. Du, J., and Frieden, C. (1998) *Biochemistry 37*, 13276−13284.
36. Korn, E. D. (1982) *Physiol. Rev. 62*, 672−737.
37. Caldwell, J. E., Heiss, S. G., Mermall, V., and Cooper, J. A. (1989) *Biochemistry 28*, 8506−8514.
38. Cooper, J. A., and Pollard, T. D. (1985) *Biochemistry 24*, 793−799.
39. Yin, H., Hartwig, J. H., Maruyama, K., and Stossel, T. P. (1981) *J. Biol. Chem. 256*, 9693−9697.
40. Wegner, A., Aktories, K., Ditsch, A., Just, I., Schoepper, B., Selve, N., and Wille, M. (1994) *Adv. Exp. Med. Biol. 358*, 97−104.
41. Oosawa, F., and Kasai, M. (1962) *J. Mol. Biol. 4*, 10−21.
42. Buzan, J. M., and Frieden, C. (1996) *Proc. Natl. Acad. Sci. U.S.A. 93*, 91−95.
43. Frieden, C. (1983) *Biochemistry 20*, 6513−6517.
44. Selden, L. A., Kinosian, H. J., and Estes, J. E. (1994) *Adv. Exp. Med. Biol. 358*, 51−57.
45. McGhee, J. D., and vonHippel, P. H. (1974) *J. Mol. Biol. 86*, 469−489.

BI011806U